 

# Study of DNA Amplification Efficiency Based on Temperature Analyses of the Moving Fluid in a Liquid-Plug Flow PCR System

**Yusuke Fuchiwaki,*[1,2] Hidenori Nagai,[2] Masato Saito,[3] and Eiichi Tamiya[3]**

[1]Health Research Institute, National Institute of Advanced Industrial Science and Technology (AIST), 2217-14 Hayashi-cho, Takamatsu, Kagawa 761-0395

[2]Health Technology Research Institute, National Institute of Advanced Industrial Science and Technology (AIST), 1-8-31 Midorigaoka, Ikeda, Osaka 563-8577

[3]Department of Applied Physics, Graduate School of Engineering, Osaka University, 2-1 Yamadaoka, Suita, Osaka 565-0871

Received May 9, 2011; E-mail: yu-fuchiwaki@aist.go.jp

Flow-through PCR devices for performing rapid and small-volume DNA amplification on a single chip have attracted great interest. Flow-through DNA amplification was performed by moving PCR solution as a liquid plug through three individual temperature zones. Since precise control of the temperature setting is the most important technique for successful DNA amplification, real-time temperature analyses of the moving fluid were investigated using a polyolefin pressure-sensitive adhesive (PPSA) film to cover the microchannel. The temperature profile at 20 °C during annealing phase was the closest to the recommended conditions for PCR compared to the profile from 55 to 20 °C, and it showed the highest amplification of the tested regimes. The microchannel design was optimized using an infrared (IR) thermal imager to significantly increase the fluorescence intensity of the amplified products. A flow time of five to six seconds per cycle resulted in a temperature profile close to the recommended thermal gradient. These studies resulted in effective findings for simple and rapid amplification by moving a PCR solution as liquid-plug on a single chip.

Polymerase chain reaction (PCR) is an exponential in vitro DNA amplification technique widely applied in biomedical and other related fields. PCR can create copies of specific fragments of DNA by cycling through three temperature zones generated by thermal cyclers. Recently, miniaturized PCR devices with microfabricated structures have been described and can be used in the field to detect target genes.[1–4] However, conventional thermal cyclers used for standard laboratory tests are large; for example, most are the size of a small kitchen appliance such as a microwave oven. The material and volume of the thermal cycler creates a large heat mass, which leads to slow thermal cycling. Furthermore, these laboratory units require that the sample be obtained in the field and then transported to a laboratory.

During the influenza pandemic in 2009, an accurate diagnosis using conventional technology required at least several hours. To quickly curtail an outbreak, rapid field detection of the target gene is needed. To meet this demand, flow-through PCR microfluidic devices are seen as a realistic micro total analysis system (μ-TAS) that could provide rapid detection in the field. Since a flow-through PCR microfluidics device was first reported by Kopp et al. in the late 1990s,[5] interest has grown in an automated PCR system that can perform all the assay steps on a single chip. In principle, PCR reagents are loaded into a long microflow channel and repeatedly carried through individual temperature zones for denaturation, extension, and annealing. This approach has several advantages, such as: 1) the heater does not require strict control of temperature, 2) rapid PCR amplification is possible due to rapid thermal cycling, and 3) it is easier to automate routine work such as injections, DNA amplification, and detection.[1,4,6–11] In addition, this approach can be applied to reverse-transcription PCR (RT-PCR) by integrating the microfluidic RT process on a single chip, as demonstrated by the rapid diagnosis of influenza.

Polymer-based PCR microfluidic devices have recently gained attention due to their low cost, easy surface modification, and the use of light, permeable materials. Many such microfluidic devices have been reported including ones utilizing PDMS (poly(dimethylsiloxane)),[4,12–14] PMMA (poly(methyl methacrylate)),[15] and PC (polycarbonate).[16,17] Recently, we fabricated flow-through PCR microfluidic devices using COP (cycloolefin polymer) resins as a substrate.[18] COP is a thermoplastic with low porosity, high heat resistance ($T_g$ of COP 480: 138 °C), low impurities, low emitted gasses, small nonspecific adsorption to fluidic channels, and the lowest water absorbency of all plastics.[19–22] These properties are very convenient for highly effective DNA amplification with flow-through PCR. High heat resistance is an absolute requirement for PCR microfluidic devices. Low porosity and low emitted gasses keep the PCR solution from evaporating. Small nonspecific adsorption results in greater yield. Furthermore, COP is highly transparent in the visible wavelength range 400–800 nm, and is less fluorescent than other polymer resins. Thus, COP has the properties required for practical, commercial application in a PCR kit.

Published on the web October 15, 2011; doi:10.1246/bcsj.20110130

Our fabricated system can realize a simple and very fast PCR in only 240 s for 40-cycle PCR.[18] Its great advantage is continuity by which one can choose the design needed. Gradient and uniformity of temperature zone are key parameters of the system; the gradient ensures correct reaction temperature and the uniformity ensures correct temperature distribution. Although temperature analyses of flow-through PCR materials have been conducted by many researchers, there are few reports providing detailed analyses focused on the temperature of the moving fluid itself.[23–27] As the fluidic speed increases, the temperature setting on the PCR chip material no longer correctly reflects the fluidic temperature. Indeed, temperature analyses of the moving fluid have never been performed for flow-through PCR devices based on polymer resins, even though these parameters are crucially important.

For the temperature analysis of a moving fluid, the use of thermotolerant and transparent thin films is desirable for the construction of the enclosed microchannel structure. Polyolefin pressure-sensitive adhesive (PPSA) thin film can be used to construct the enclosure simply by weighing it on COP substrate and then microchannels can be cut using a CAD program. The temperature of the channel close to the moving fluid can be analyzed with an infrared (IR) thermal imager; consequently, PPSA film allows uniform bonding and exhibits thermotolerant properties. Currently, the fabrication and proper use of chip devices requires technical knowledge, experience, and skill. In contrast, the fabrication of this PCR chip device is a relatively foolproof operation.

PCR chips are expected to make large contributions in various fields such as prevention of infectious disease, individual medicine, and bioterrorism defense. The results of this study provide the most recent findings for precise control of temperature setting and will accelerate an effective application of flow-through PCR on a single chip.

## Experimental

**Reagents and Materials.** The following reagents for PCR were obtained from a CycleavePCR Core kit from TaKaRa: 10 × CycleavePCR buffer, dNTP mixture (2.5 mM), Mg solution (25 mM), positive control primer mix, positive control probe, Tli RNase H II (200 U $\mu L^{-1}$), and Takara Ex Taq HS (5 U $\mu L^{-1}$), $dH_2O$. The positive controls in the CycleavePCR Core kit were used as the target genes for all PCR analyses. This kit employs Cycling Probe Technology, a highly sensitive detection method using a combination of chimera probes (composed of RNA and DNA) and RNase H. The specific sequence of the target gene can be detected efficiently after amplification, with the amplification efficiency being estimated from the obtained fluorescence intensity.

COP ZEONEX 480 was purchased from Zeon Corporation, Japan. COP is a 2-mm-thick thermoplastic biocompatible polymer. The characteristics of this heat-resistant resin are comparable with PC and PS (polystyrene). COP is superior for containing aqueous solutions due to its low water absorption coefficient. PPSA film (Model number: 9795) was purchased from CS-LABO, Japan.

**Fabrication of Flow-Through PCR Microfluidics Device.** The microflow channel on the COP substrate was fabricated by cutting microchannels with a numerical control (NC) machine, which was automatically operated by CAD programs. The NC machine was manufactured by PMT Corporation (Micro MC-2, Japan) and the milling cutter used a ball-end mill with radius 200 μm. Cutting feed rate was operated at one millimeter per second and spinning rate was operated at 8000 revolutions per second. Chip fabrication was completed by weighing the PPSA film on the COP substrate (Figure 1a). The microfluidic device was designed to perform 40 thermal cycles for amplification. The PCR chip device was 80 mm long and 50 mm wide. The heater and cooler were composed of aluminum blocks $15 \times 10 \times 100\,mm^3$. The heat-transfer aluminum block contained a heat conductor and temperature sensor (Kyushu-Nissho Co., Fukuoka, Japan). The aluminum block for cooling was in contact with a Peltier cooling element (SPE-UC-100, SAKAGUCHI E.H Corporation). The chip device was placed on the aluminum blocks, and the PCR solution containing the target genes was introduced through the inlet with a syringe pump. The blocks were configured so that the PCR solutions passed through three different temperature zones repeatedly (Figure 1b). The aluminum block temperatures for extension and denaturation were set at 72 and 95 °C, respectively. The optimum temperature for the annealing zone was thought to be less than 60 °C. The PCR products were collected in microplate wells and their fluorescence intensities were detected with a fluorescence microplate reader (Fluoroskan Ascent, Thermo Scientific). The moving fluid was visualized by IR imaging using a thermal imager (Ti10, Fluke Corporation, U.S.A.).

## Results and Discussion

**Temperature Analysis of Microfluids-Based IR Imaging.** Flow-through PCR systems amplify DNA by continuously flowing the PCR reagents through discrete temperature zones for denaturation, extension, and annealing. However, such continuous flow requires complex operation and a large quantity of PCR solution. In addition, continuous flow devices must circumvent turbulent flow caused by bubble generation in the denaturation zone microchannel (95 °C). We recently reported a liquid plug flow-through PCR method[18] which flows only a small amount of PCR solution (Figure 2). The PCR reagents pass rapidly through the area where air bubbles could form before any bubbles can be generated to destabilize the flow. This approach allows rapid flow and simple PCR operation. However, the rapid flow makes it difficult to keep the required thermal gradient in the fluid. This is due to the inner pressure in the microchannel, and makes the application of the liquid-plug flow-through PCR system impractical. The precise control of the temperature setting is imperative for successful amplification. In particular, this system must carefully examine correct temperature gradient and uniformity because of realizing by moving a PCR solution through the individual temperature zones. Therefore, we focused on optimizing temperature analysis close to the moving fluid by controlling characteristics of the PPSA film such as depth, thickness, thermal tolerance, transparency, and uniform adhesion.

The temperature distribution along the PPSA film was investigated using IR imaging. The gap between the aluminum blocks was set to prevent heat transmission. The denaturation, extension, and annealing temperatures were set to 95, 72, and 20 °C, respectively. Deviations in the temperature distribution

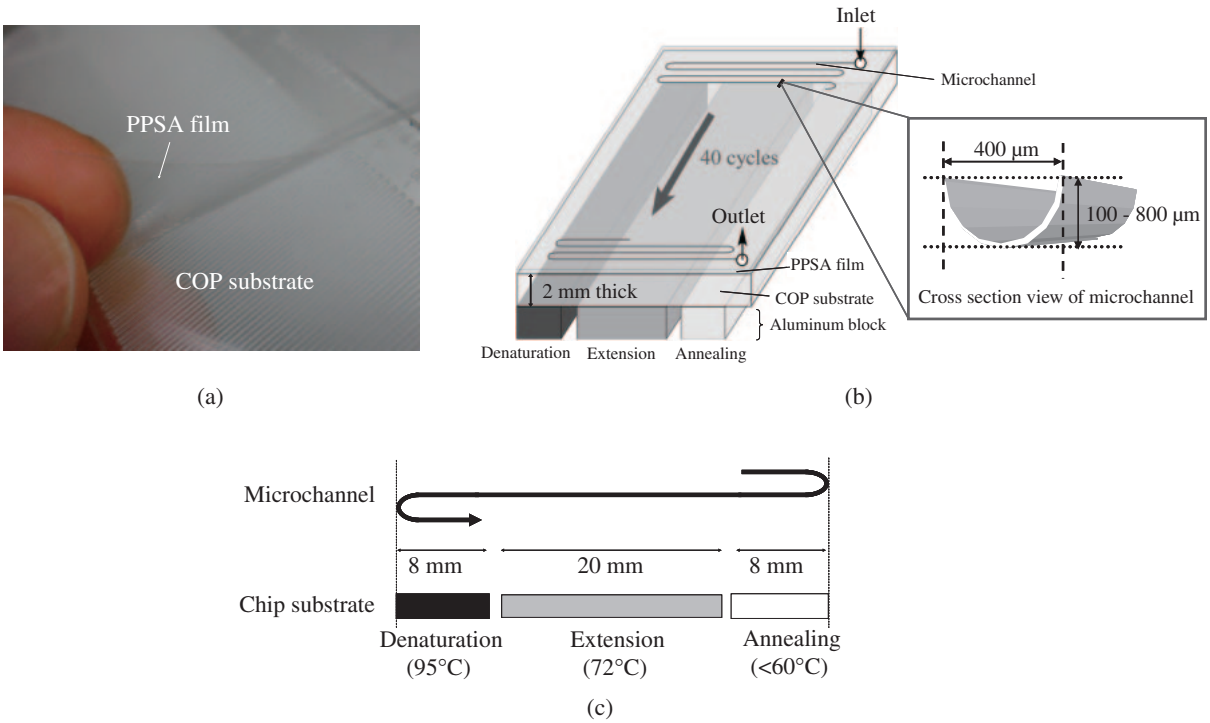


**Figure 1.** The flow-through PCR microfluidic device made of COP substrate and PPSA film: (a) Photo of the flow-through PCR microfluidic device, (b) diagrammatic illustration of the flow-through PCR microfluidic device, and (c) configuration of heating in three temperature zones.

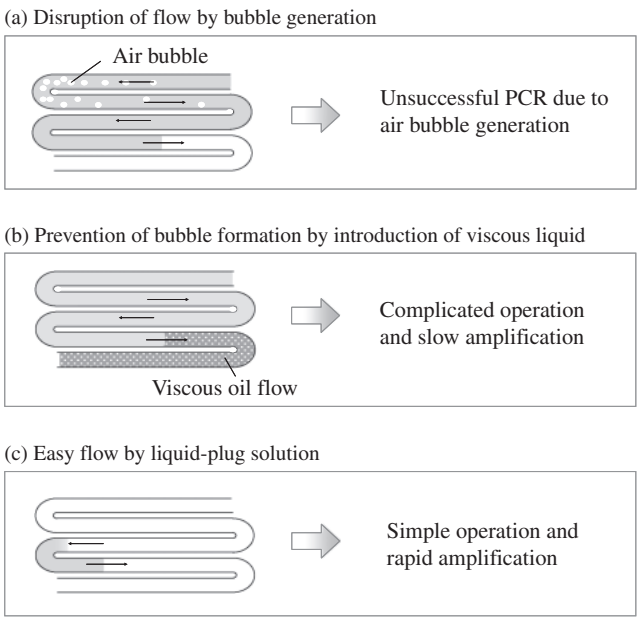


**Figure 2.** Methodology for flow-through PCR using a microfluidics system.

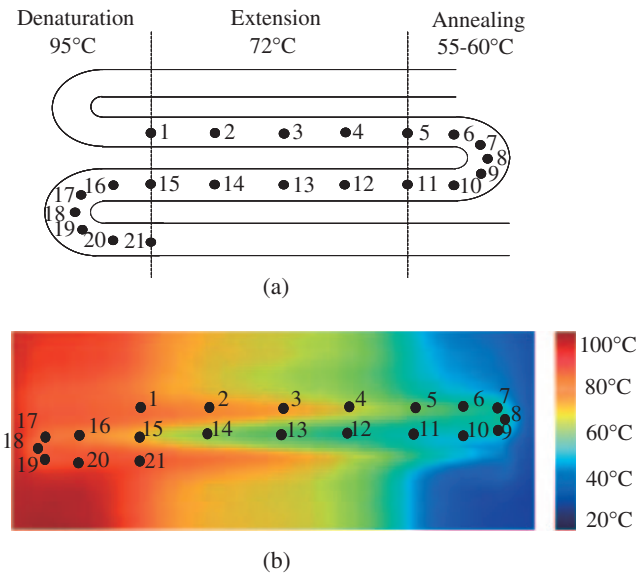


**Figure 3.** Temperature analysis at a point marked on the PPSA film: (a) Measuring points along the microchannel and (b) measuring points for infrared imaging when the solution is flowing in the microchannel.

were approximately 1.0–2.2 °C, which fall in the allowable range. IR imaging of the thinner PPSA film allowed analysis of the temperature of the microfluidics (Figure 3). The measuring points were marked along the microchannel as shown in Figure 3a. The thermal distribution in the microfluidics could be profiled by IR imaging, as shown in Figure 3b, and the conditions for efficient PCR amplification were investigated.

Liquid-plug flow is sensitive to the inner pressure derived from each temperature zone. Thus, the thermal settings must be determined to obtain a correct temperature gradient for PCR. The residual time and flow rate changed in each temperature zone (Figure 4a). The residual time was longest between measuring points 11–15 because the inner pressure caused by the high temperature in the denaturation zone reduced the flow

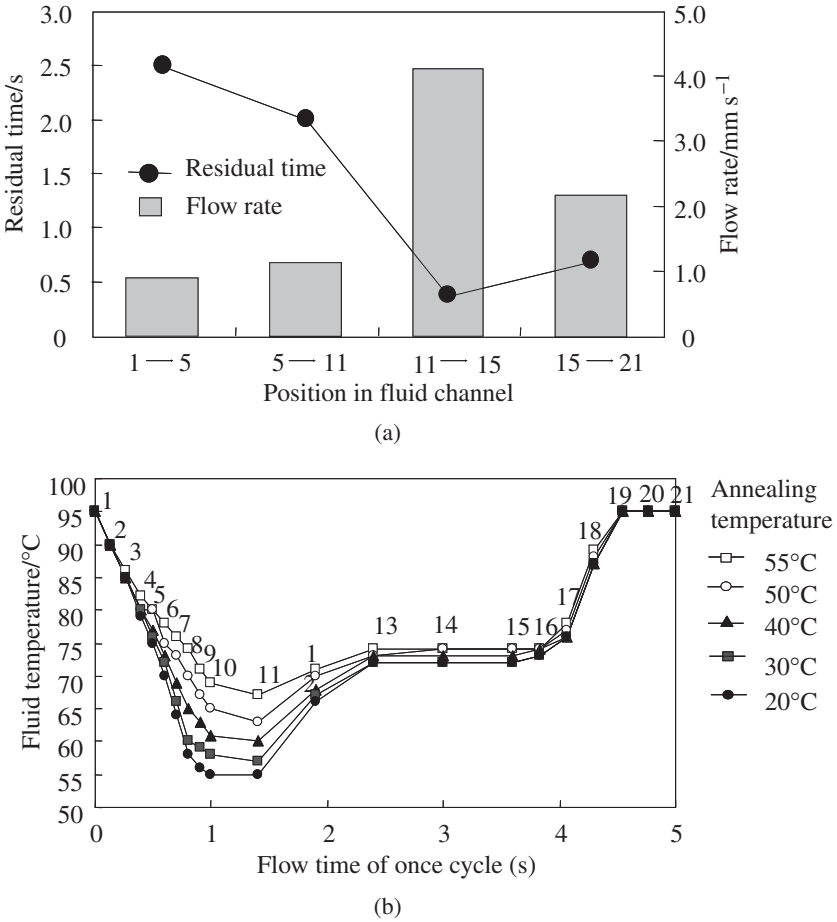


**Figure 4.** Flow speed and temperature distribution along the microchannel during flow: (a) Residual time and flow rate in each thermal zone and (b) profiling of temperature distribution relative to the annealing zone from 20 to 55 °C.

**Table 1.** Relationship between Fluorescence Intensity and Temperature of Annealing[a)]

| | Temperature of annealing/°C | | | | |
|---|---|---|---|---|---|
| | 55 | 50 | 40 | 30 | 20 |
| Fluorescence intensity | 0.29 ± 0.18 | 0.32 ± 0.21 | 1.07 ± 0.56 | 2.77 ± 0.29 | 3.27 ± 0.32 |

a) Volume: 1 µL, flow velocity: 6 s per cycle.

speed. In contrast, the residual time was the shortest between measuring points 1–5. These results indicate that the heating time in the extension zone was longer than anticipated, but the cooling time from denaturation to annealing was shorter. The time ratios typically recommended for PCR amplification are 1:3:2 for denaturation:extension:annealing. An increased extension zone is very beneficial for PCR amplification, but in our device the annealing zone between points 5–11 was short.

Since the fluidic temperature cools by 55 °C in a short time, a temperature profile based on IR imaging was constructed to investigate the optimal temperature setting for the annealing zone (Figure 4b). As the temperature decreased from 55 to 20 °C, the profile approached the recommended conditions. The fluorescence intensity of the amplified products began to increase below 40 °C and maximized at 20 °C (Table 1). The fluorescence intensities at 50 and 55 °C were similar to that of the negative control not containing target genes, where you expect to see no result.

Since the gradient and distribution of temperature were affected by the speed of the flowing plug, the temperature profile was examined in relation to the flow speed for one complete thermal cycle, lasting between 1 and 10 s (Figure 5). At a faster flow speed of 1–2 s per cycle, there was insufficient temperature difference between the denaturation and annealing zones. In contrast, the temperature of the annealing area cooled too much at a slow speed of 7–10 s per thermal cycle. Increased cooling increases the risk of creating primers or dimers as residual products. The temperature profiling indicated that approximately 5–6 s per cycle provides the temperature gradient recommended for PCR.

**Study of Microchannel Design Based on IR Imaging.** In the serpentine, rectangular microchannel of a flow-through PCR microfluidics chip, PCR efficiency is greatly influenced by the design of the microchannels because the design affects heat transfer to the flowing fluid. Specifically, the distance between microchannels influences the continuous heat transfer

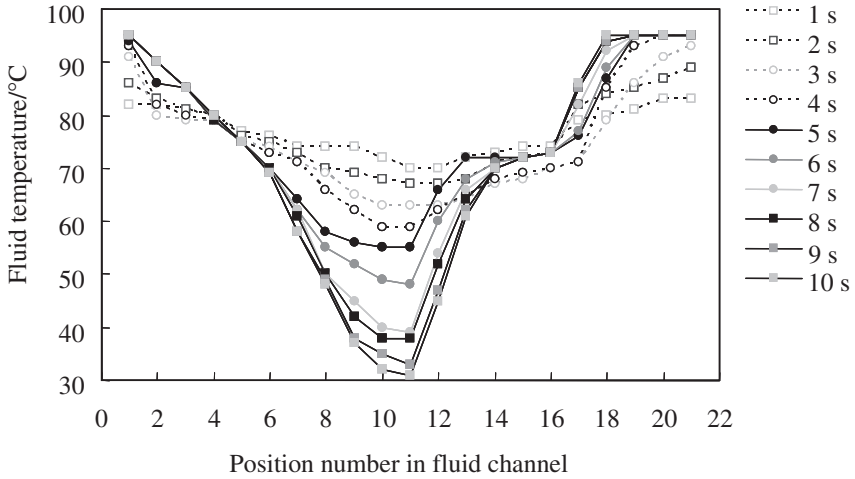


**Figure 5.** Temperature distribution along the microchannel relative to different times per cycle, from 1 to 10 s. Annealing temperature was set at 20 °C.

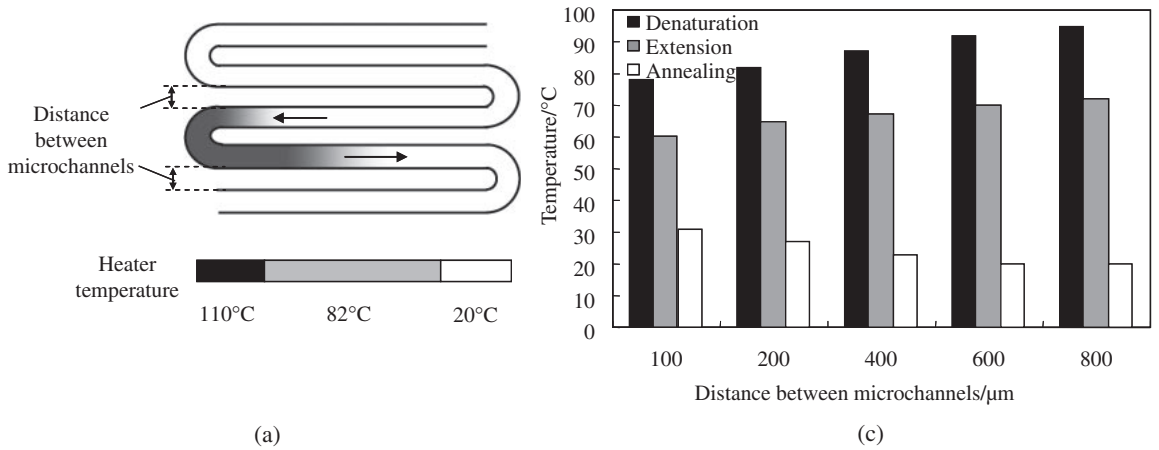


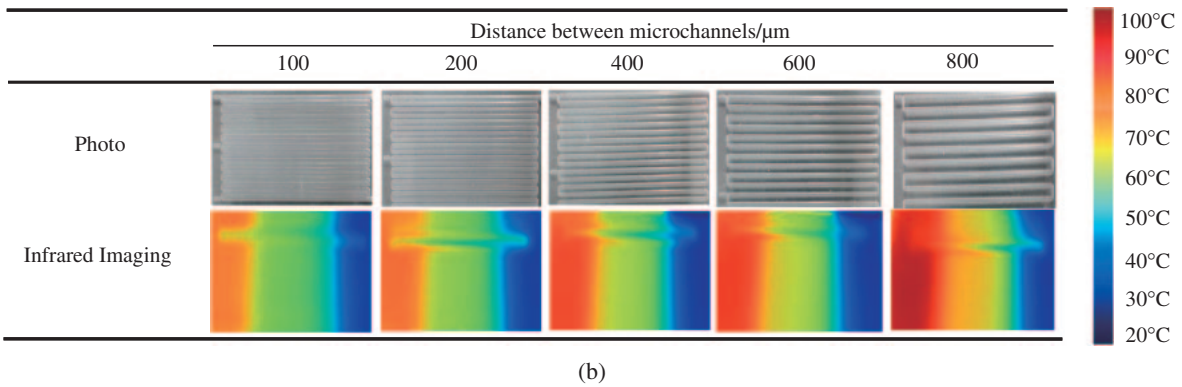


**Figure 6.** Investigation of optimum distance between the microchannels based on IR. (a) Illustration of the microchannel, (b) IR imaging for each distance between the microchannels. (c) Temperature in the three temperature zones vs. the distance between the microchannels.

to the flowing fluid (Figure 6a). IR imaging and the temperature on the chip surface were investigated at various distances along the microchannel (Figures 6b and 6c). As the distance decreased, the heater temperature was not reflected in the chip device because the gap space in the microchannel was greater than the distance in the heater element, and the microchannel design showed insufficient heat conductivity. Superior heat-transfer capability of the chip material enables continuous thermal control of the fluidic PCR reagents, allowing PCR to be efficiently conducted on a single chip. When the fluidic reagents pass through the microchannel, the chip material was also cooled by heat transfer from the fluid. This cooling changes the temperature of the internal wall of the adjacent microchannel. If the distance between microchannels is in-

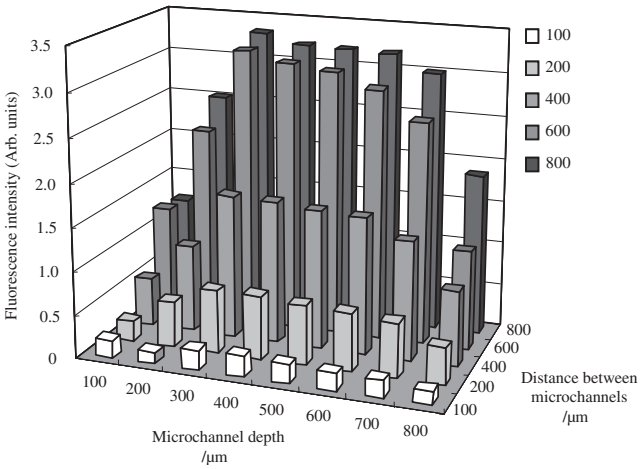


**Figure 7.** Comparison of the fluorescence intensities obtained by rapid flow-through PCR relative to channel depth and the distance between microchannels. Flow speed was set at 6 s per cycle and the volume was 1 μL.

sufficient, it is difficult to immediately restore the thermal setting for PCR due to heat transmission to the fluidic PCR reagents. Thus, we determined that a distance of 800 μm between microchannels is required to produce an accurate temperature gradient.

Nonuniform thermal distribution in the horizontal direction affects PCR efficiency. The thickness of the chip was 2 mm, and the temperature difference between the upper surface and the surface contacting the aluminum block was approximately 10 °C when the surface of the aluminum block was 110 °C. This difference was large enough to compromise uniform heat transfer to the fluid, so the influence of microchannel depth and the distance between microchannels on PCR efficiency was investigated (Figure 7). As the distance between microchannels increased, the fluorescence intensities increased and became maximum at distances greater than 800 μm, whereas at 100 μm, the intensities were almost the same as that of the negative control. However, when the channel depth was in the range of 300–700 μm, the fluorescence intensity was large. Fluidic evaporation in the microchannel was seen if the channels were 100–200 μm deep because the PCR reagents in the denaturation zone had to pass through the narrow microchannel and be exposed to almost boiling temperatures. Destabilized flow was observed if the microchannels were 800 μm deep because the bottom of the microchannel was near the aluminum block, which was at 110 °C.

The heat transfer rate of COP is higher than that of glass and PDMS, which are commonly used materials for PCR chips. It is important to determine optimal microchannel design for rapid flow in other chip materials. In this study, the correct temperature settings and the optimal microchannel design for PCR amplification were determined based on IR imaging of PPSA film surface. As a result, 40-cycle PCR was performed, requiring 6 s per cycle. The amplification efficiency of the products was approximately 80% that of a commercially available PCR instrument, a significant improvement over previous reports.[3,18,28–31] The amplification efficiency of this study succeeded in increasing about 25% from previous report.[18]

In concluding, we should note that it is crucially important to study the IR thermal imaging close to moving fluid and the microchannel design for widespread practical application of the technology. Since the first reports by Kopp et al. in the late 1990s,[5] there is growing interest in flow-through PCR systems that can perform all the assay steps on a single chip. We truly believe that the results of this study will have considerable impact on rapid field detection based on PCR.

## Conclusion

IR imaging of the PPSA film surface allowed temperature profiling of the PCR and subsequent detailed analyses of the microfluidic temperature. The profiling showed that the closest recommended condition for PCR was obtained when the annealing temperature was set at 20 °C. The temperature distribution was investigated in the range from 1 to 10 s per cycle and showed that the recommended thermal gradient was obtained in approximately 5–6 s. The microchannel design was optimized using an IR imager and a significant increase in fluorescence intensity was achieved, indicating product amplification. Good PCR efficiency was obtained when the distance between the microchannels was 800 μm and the depth of the microchannel was between 300–700 μm for a 2-mm-thick COP chip device. When PCR amplification was completed in 40 thermal cycles at 6 s per cycle, the amplification efficiency of the products was approximately 80% that of a commercial PCR instrument, an impressive improvement over previously reported PCR chips. Thus, this flow-through PCR chip holds promise in areas such as clinical applications and the reduction of bioterrorism threats.

This work was supported by the Grant of Science Technological Project for Safety and Security and was sponsored by the Ministry of Education, Culture, Sports, Science and Technology of Japan. The authors highly appreciate Dr. Shin-ichi Wakida's contribution to this study.

## References

1 C. Zhang, D. Xing, *Nucleic Acids Res.* **2007**, *35*, 4223.
2 E. A. Ottesen, J. W. Hong, S. R. Quake, J. R. Leadbetter, *Science* **2006**, *314*, 1464.
3 P. Neuzil, C. Zhang, J. Pipper, S. Oh, L. Zhuo, *Nucleic Acids Res.* **2006**, *34*, e77.
4 T. Fukuba, T. Yamamoto, T. Naganuma, T. Fujii, *Chem. Eng. J.* **2004**, *101*, 151.
5 M. U. Kopp, A. J. de Mello, A. Manz, *Science* **1998**, *280*, 1046.
6 E. T. Lagally, P. C. Simpson, R. A. Mathies, *Sens. Actuators, B* **2000**, *63*, 138.
7 I. Schneegaß, J. M. Köhler, *Rev. Mol. Biotechnol.* **2001**, *82*, 101.
8 P. Belgrader, C. J. Elkin, S. B. Brown, S. N. Nasarabadi, R. G. Langlois, F. P. Milanovich, B. W. Colston, Jr., G. D. Marshall, *Anal. Chem.* **2003**, *75*, 3446.
9 P. J. Obeid, T. K. Christopoulos, *Anal. Chim. Acta* **2003**, *494*, 1.
10 J. P. Ferrance, Q. Wu, B. Giordano, C. Hernandez, Y. Kwok, K. Snow, S. Thibodeau, J. P. Landers, *Anal. Chim. Acta* **2003**, *500*, 223.

11 C. Zhang, J. Xu, W. Ma, W. Zheng, *Biotechnol. Adv.* **2006**, *24*, 243.

12 J. W. Hong, T. Fujii, M. Seki, T. Yamamoto, I. Endo, *Electrophoresis* **2001**, *22*, 328.

13 T. Nakayama, Y. Kurosawa, S. Furui, K. Kerman, M. Kobayashi, S. R. Rao, Y. Yonezawa, K. Nakano, A. Hino, S. Yamamura, Y. Takamura, E. Tamiya, *Anal. Bioanal. Chem.* **2006**, *386*, 1327.

14 T. Nakayama, H. M. Hiep, S. Furui, Y. Yonezawa, M. Saito, Y. Takamura, E. Tamiya, *Anal. Bioanal. Chem.* **2010**, *396*, 457.

15 D.-S. Lee, S. H. Park, H. Yang, K.-H. Chung, T. H. Yoon, S.-J. Kim, K. Kim, Y. T. Kim, *Lab Chip* **2004**, *4*, 401.

16 Y. Liu, C. B. Rauch, R. L. Stevens, R. Lenigk, J. Yang, D. B. Rhine, P. Grodzinski, *Anal. Chem.* **2002**, *74*, 3063.

17 J. Yang, Y. Liu, C. B. Rauch, R. L. Stevens, R. H. Liu, R. Lenigk, P. Grodzinski, *Lab Chip* **2002**, *2*, 179.

18 Y. Fuchiwaki, M. Saito, S. Wakida, E. Tamiya, H. Nagai, *Anal. Sci.* **2011**, *27*, 225.

19 K. Faure, M. Albert, V. Dugas, G. Crétier, R. Ferrigno, P. Morin, J.-L. Rocca, *Electrophoresis* **2008**, *29*, 4948.

20 Y. Luo, X. Wang, F. Yang, *J. Mater. Process. Technol.* **2008**, *208*, 63.

21 J. Mizuno, H. Ishida, S. Farrens, V. Dragoi, H. Shinohara, T. Suzuki, M. Ishizuka, T. Glinsner, F. P. Lindner, S. Shoji, in Digest of Technical Papers of the 2005 International Conference on Solid-State Sensors, Actuators and Microsystems (Transducers 2005), June 5–9, Seoul, Korea, **2005**.

22 H. Shinohara, T. Suzuki, F. Kitagawa, J. Mizuno, K. Otsuka, S. Shoji, *Sens. Actuators, B* **2008**, *132*, 368.

23 F. Kitagawa, T. Suzuki, J. Mizuno, S. Shoji, K. Otsuka, in Digest of Technical Papers of the 10th International Conference on Miniaturized Systems for Chemistry and Life Sciences (μTAS2006), November 5–9, Tokyo, Japan, **2006**.

24 K. Sun, A. Yamaguchi, Y. Ishida, S. Matsuo, H. Misawa, *Sens. Actuators, B* **2002**, *84*, 283.

25 Q. Zhang, W. Wang, H. Zhang, Y. Wang, *Sens. Actuators, B* **2002**, *82*, 75.

26 J. El-Ali, I. R. Perch-Nielsen, C. R. Poulsen, D. D. Bang, P. Telleman, A. Wolff, *Sens. Actuators, A* **2004**, *110*, 3.

27 W. Yan, L. Du, J. Wang, L. Ma, J. Zhu, *Sens. Actuators, B* **2005**, *108*, 695.

28 C.-Y. Shih, Y. Chen, Y.-C. Tai, *Sens. Actuators, A* **2006**, *126*, 270.

29 Y.-C. Lin, M.-Y. Huang, K.-C. Young, T.-T. Chang, C.-Y. Wu, *Sens. Actuators, B* **2000**, *71*, 2.

30 S.-H. Han, D.-B. Lee, D.-W. Lee, E.-H. Kim, B.-S. Yoon, *J. Invertebr. Pathol.* **2008**, *99*, 8.

31 J. A. Kim, J. Y. Lee, S. Seong, S. H. Cha, S. H. Lee, J. J. Kim, T. H. Park, *Biochem. Eng. J.* **2006**, *29*, 91.